additional data are required to evaluate this hypothesis.

Conclusions. The time-resolved laser absorption spectroscopic method described here offers a general approach for studying the photodissociation dynamics of transition-metal carbonyls and the spectroscopy and chemical kinetics of the coordinatively unsaturated species formed as a result of photodissociation. In the present article, we have applied this method in characterizing the primary and secondary processes which occur following the photoactivation of $Cr(CO)_6$ at 249 nm.

Our results demonstrate that photoactivated $Cr(CO)_6$ rapidly decays to $Cr(CO)_5$ and CO. The nascent CO product is translationally, as well as rovibrationally, excited, and the $Cr(CO)_5$ product is formed with sufficient internal energy to decay to $Cr(CO)_4$ and CO. Both dissociation reactions occur within 10^{-7} s after the photoactivation step. The $Cr(CO)_4$ and CO formed via the unimolecular dissociation of $Cr(CO)_5$ are both relatively cold, and the $Cr(CO)_4$ product is stable with respect to further unimolecular decay. $Cr(CO)_4$ is observed to undergo association with $Cr(CO)_6$ on every gas kinetic collision, forming the binuclear complex $Cr_2(CO)_{10}$. This species is stable to times on the order of at least 10^{-3} s. Both $Cr(CO)_4$ and $Cr(CO)_5$ are found to recombine with CO at a rate corresponding to one in ten gas kinetic collisions, forming $Cr(CO)_5$ and $Cr(CO)_6$, respectively. Our results demonstrate that under appropriate conditions, reactive species such as $Cr(CO)_4$, $Cr(CO)_5$, and $Cr_2(CO)_{10}$ can be generated in the gas phase in yields sufficient for the study of their spectroscopy and kinetics.

Acknowledgment is made to the donors of the Petroleum Research Fund, administered by the American Chemical Society, for partial support of this work. Additional support has been provided by the National Science Foundation through Grant NSF CHE82-06897.

Registry No. $Cr(CO)_6$, 13007-92-6; $Cr(CO)_5$, 26319-33-5; $Cr(CO)_4$, 56110-59-9; $Cr_2(CO)_{10}$, 95387-63-6; CO, 630-08-0.

Molecular Mechanical Studies of Inclusion of Alkali Cations into Anisole Spherands

Peter A. Kollman,* Georges Wipff,† and U. Chandra Singh

Contribution from the Department of Pharmaceutical Chemistry, University of California, San Francisco, San Francisco, California 94143. *Received December 22, 1983*

Abstract: We present molecular mechanical studies of host spherands **1**, **2**, and **3** and their complexes with Li^+, Na^+, and K^+ guests. Even though such an approach is quite simple, we show that it is capable of giving interesting insight into host/guest complexation. Specifically, we calculate a high selectivity of **1** for Li^+ and Na^+ complexation compared to that of K^+, in agreement with experiment. The difference between $-\Delta E$ for complexation of Na^+ compared to K^+ is much larger with **1** (41 kcal/mol) than with 18-crown-6 (**4**) (8 kcal/mol). This dramatic difference clearly shows why **1** has no thermodynamic tendency to bind K^+. Decomplexation of the unsolvated cations from the cavity of **1** has been simulated by moving Li^+, Na^+, and K^+ along the threefold axis out of the molecule; this lead to ~25 kcal/mol higher energies for Li^+ and Na^+ but ~55 kcal/mol higher energy for K^+. Moving the cations further along the axis of **1** and energy refining causes Li^+ and Na^+ to return to the center of the cavity; K^+, on the other hand, remains on the outside of the cavity with an energy 18 kcal/mol lower than that found at the model "transition state". The calculated free energy differences in complexation of Li^+ and Na^+ with **1** and **2** are 13.6 and 15.6 kcal/mol, respectively, qualitatively consistent with the observed free energy differences of >12.6 and 12.6 kcal/mol, respectively. We present normal mode analyses and entropy calculations on **1** and **2** and their complexes, which help to further elucidate the nature of these complexes. Calculations on spherand **3a** lead to a relative free energy of Li^+ complexation which is qualitatively consistent with the experimental observation that the complexation free energy of **3a** is between that of **1** and **2**. Another conformation of this molecule, **3b**, is calculated to have a higher Li^+ affinity even than **1**, which has the highest experimentally observed Li^+ affinity. This conformation is calculated to be much more stable than **3a**, and reaction pathway calculations suggest that **3a** is a kinetically trapped conformation. These predictions have been borne out by experiments (see Note Added in Proof).

Spherands are very interesting ionophores, which differ from crowns, cryptands, and natural ionophores in that they are "fully organized" for cation complexation during synthesis rather than undergoing conformational changes in the presence of cation. Cram et al.,[1,2] Lein and Cram,[3] and Trueblood et al.[4] have presented the synthesis, thermodynamics, and kinetics of binding and X-ray crystal structures of a number of spherands and have demonstrated that spherand **1** has the highest binding affinity for Li^+ and Na^+ of this class of structures, larger than the affinity of the best simple cryptand binders for Li^+ and Na^+ (by $\sim 10^4$ and 10^2, respectively[2]). The rather dramatic difference in affinity of Li^+ and Na^+ for **1** compared to **2** is also interesting; replacement of a single OCH_3 by H reduces the association constant for binding of cation by $\sim 10^9$ for both cations. Another very interesting result is the complete lack of (measurable) affinity of **1** for K^+, in that **1** will extract trace amounts of Na^+ and Li^+ from reagent grade KOH when mixed with that base.[1]

We have been interested in modeling cation–ionophore interactions for some time and have recently presented the first extensive molecular mechanics study[5] of an ionophore *and* its cation complexes. The results of that study were encouraging, in that a rather simple simple model was able to account for the relative stabilities of 18-crown-6 conformations in the absence of cation

† Institut de Chimie, BP 296/R8, 67008 Strasbourg, France.

(1) Cram, D. J.; Kaneda, T.; Helgeson, R. C.; Lein, G. M. *J. Am. Chem. Soc.* **1979**, *101*, 6752.
(2) Cram, D. J.; Lein, G. M.; Kaneda, T.; Helgeson, R. C.; Knobler, C. B.; Maverik, E.; Trueblood, K. N. *J. Am. Chem. Soc.* **1981**, *103*, 6228.
(3) Lein, G. M.; Cram, D. J. *J. Chem. Soc., Chem. Commun.* **1982**, 301.
(4) Trueblood, K. N.; Knobler, C. B.; Maverick, E.; Helgeson, R. C.; Brown, S. B.; Cram, D. J. *J. Am. Chem. Soc.* **1981**, *103*, 5594.
(5) Wipff, G.; Weiner, P.; Kollman, P. *J. Am. Chem. Soc.* **1982**, *104*, 3249.

0002-7863/85/1507-2212$01.50/0

Chart I

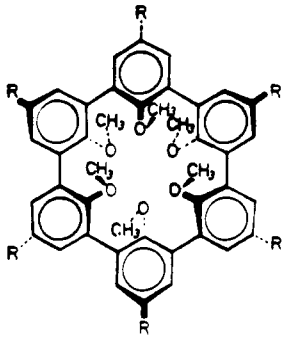

(1a) R = CH_3
(1b) R = H

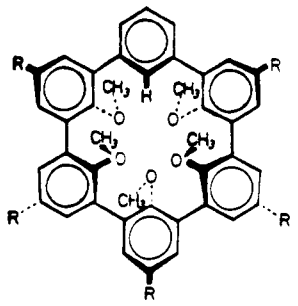

(2a) R = CH_3
(2b) R = H

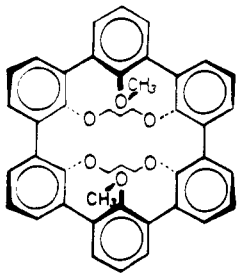

(3a)

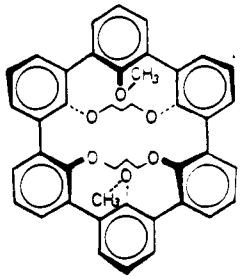

(3b)

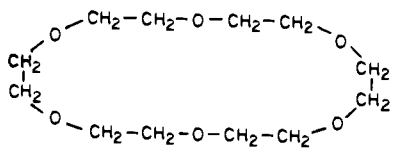

(4)

and in the presence of Na^+, K^+, Rb^+, and Cs^+ (*structural flexibility*), the relative binding affinities of different cations (*ligand specificity*), and the much greater binding affinity of cations of 18-crown-6 than to pentaglyme (*macrocyclic effect*). We thus sought to extend our calculations to the spherands, where the structural flexibility is far less, almost non-existent, the ligand specificity far greater, and the macrocyclic effect similar in nature. In this study we wish to show why **1** has a much higher affinity to Li^+ and Na^+ than to K^+ and why Li^+ and Na^+ have a dramatically higher affinity to **1** than to **2**. We also wish to characterize the normal modes of vibration of **1**, **2**, and their cation complexes, as well as using these frequencies to enable calculations of the gas-phase entropies, enthalpies, and free energies of cation complexation to **1** and **2**. Third, we wish to compare how well this very simple model reproduces the observed crystal structures of **1** and its Li^+ and Na^+ complexes. Finally, we wish to compare the properties of ionophores **3a** and **3b**, one of which (**3a**) has been characterized experimentally.

We must stress at the outset how simple and crude our theoretical approach is, compared to quantum mechanical methods. Although it is reasonably well-accepted that such molecular mechanical calculations can give a reliable representation of molecular geometries and conformational energies of organic molecules,[6] the application of such an approach to study the energetics of ionophore–ion interactions requires some optimism and luck. Our prior calculations on 18-crown-6.M^+ complexes suggest that such optimism is not totally unjustified, and it is important to establish whether a similar approach can be successful on another ionophore system.

(6) Burkert, U.; Allinger, N. L. "Molecular Mechanics"; American Chemical Society; Washington, D.C., 1982.

Table I. Additional Force-Field Parameters Used in the Study of **1–3** and Their Metal Complexes[5]

Bond Stretching Terms		
	k_b[a]	r_0, Å
$C(sp^2)$–$C(sp^2)$ (aromatic)	450	1.40
$C(sp^2)$—$C(sp^2)$ortho	300	1.51
$C(sp^2)$—H	300	1.08
$C(sp^2)$—$O(sp^3)$	300	1.36

Bond-Bending Terms		
	k_θ[b]	θ_0 (deg)
$C(sp^2)$—$O(sp^3)$—$C(sp^3)$	46.5	113
X—$C(sp^2)$—$X(sp^2)$	70.0	120

Torsional Terms			
	$k_{d,2}$[c]	$k_{d,3}$	γ (deg)
X—$C(sp^2)$–$C(sp^2)$—X	30.0		180
X—$C(sp^2)$—$C(sp^2)$—X	0.0		180
X—$C(sp^2)$—$O(sp^3)$—X	5.0		180

Nonbonded Terms[d]			
atom	α (Å^3)	Neff	R_i^0 (Å)
Li	0.20	3.0	1.0

[a] kcal/(mol Å^2). [b] kcal/(mol rad^2). [c] kcal/mol. [d] The relation between α (polarizability), Neff (number of effective electrons), radius (R_i^0), and the 6–12 parameters A and B is given in ref 7.

Methods

Our calculations used the same force field as previously employed in our study of 18-crown-6;[5] all degrees of freedom were energy refined by using analytical derivatives in Cartesian coordinates with the program AMBER.[7] However, there are several atom, bond, angle, and dihedral types which were not used in the previous study and they are listed in Table I, which follows the same format at Table X in ref 5. Where available, the parameters came from analogous parameters used in simulations on nucleic acids[9] and proteins[10] (for example, the use of 300 kcal/(mol Å^2) for single bond and 450 kcal/(mol Å^2) for aromatic bond stretching force constants, 70 kcal/(mol rad^2) for sp^2 and 46.5 kcal/(mol rad^2) for sp^3 bond bending force constants and a torsional constant for rotation around aromatic bonds which leads to a barrier which is $\sim^1/_2$ the ethylene rotational barrier). The equilibrium bond length and angle values, r_b and θ_b, came from experimental values on reasonable reference compounds (e.g., θ_b = 113° for $(C(sp^2)$–O–CH_3 in anisole).[11] We used a united atom force field (no C–H hydrogens explicitly included) with the exception of the C–H group replacing the OCH_3 when one goes from **1** to **2**. Most of our calculations were carried out on **1b** and **2b**, and we carried out calculations on **1a**, **2a**, and their Li^+ complexes to confirm that the interaction energy and structure were essentially identical with those of **1b** and **2b**.

The only torsional parameters worthy of comment are out 5.0 kcal/mol X–$C(sp^2)$–$O(sp^3)$–X rotational barrier, which, as we have shown in calculations on daunomycin,[12] leads to an energy difference between planar and perpendicular conformations of anisole of ~2 kcal/mol, in reasonable agreement with experiment[13] and our 0 kcal/mol rotational barrier in X–$C(sp^2)$–$C(sp^2)$–X, which leads to a minimum energy angle

(7) Scott, R. A.; Scheraga, H. A. *J. Chem. Phys.* **1966**, *45*, 2091.
(8) Weiner, P.; Kollman, P. *J. Comp. Chem.* **1981**, *2*, 287.
(9) Kollman, P.; Weiner, P.; Dearing, A. *Biopolymers* **1981**, *20*, 2583.
(10) Blaney, J. M.; Weiner, P. K.; Dearing, A.; Kollman, P. A.; Jorgensen, E. C.; Oatley, S. J. Burridge, J. M.; Blacke, C. C. F. *J. Am. Chem. Soc.* **1982**, *104*, 6424.
(11) This is the experimental angle for the COH angle in phenol and leads to reasonable angles for anisole and methoxy benzenes, as evidenced in ref 9.
(12) Brown, S.; Weiner, P.; Kollman, P. *Biochim. Biophys. Acta* **1982**, *717*, 49.
(13) Anderson, G.; Kollman, P.; Domelsmith, L.; Houk, K. *J. Am. Chem. Soc.* **1979**, *101*, 2344.

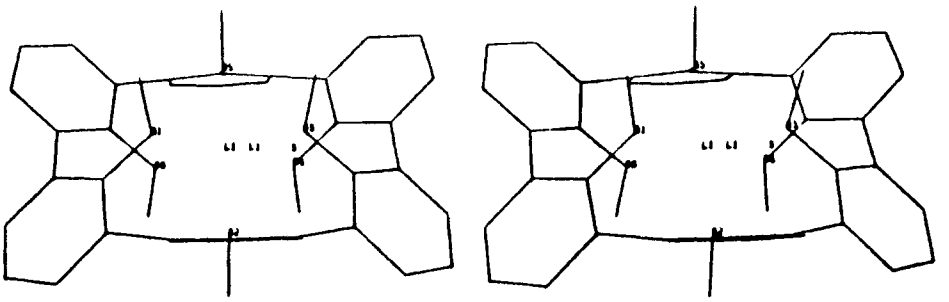

Figure 1. Stereo drawing of energy-refined Li^+/**1b**. Note that the calculated Li^+ location is the Li on the left.

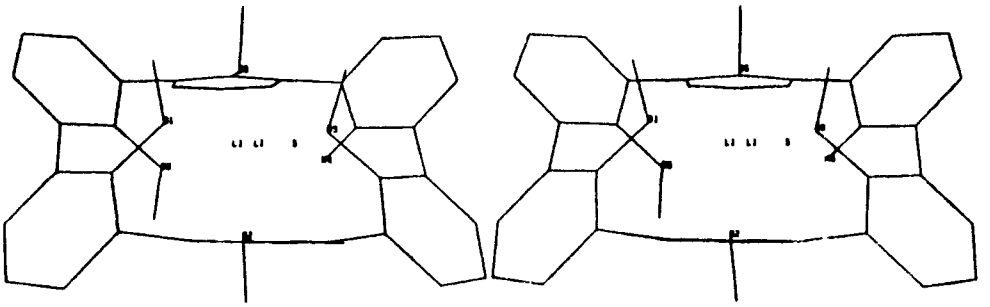

Figure 2. Stereo drawing of energy-refined Li^+/**2b**.

of ~90 for biphenyl[14] with the 0° conformation 4.4 kcal/mol higher. We also carried some refinements on biphenyl with larger X-C(sp^2)-C(sp^2)-X parameters, and a $k_{d,2}$ = 1.5 kcal/mol, which led to a minimum energy angle of 66° and a barrier of 1.4 kcal/mol for rotation through the ϕ = 0 conformation. Using $k_{d,2}$ = 3.0 kcal/mol led to a planar biphenyl minimum energy conformation. Thus, to approximately reproduce the observed nonplanar conformation of bipheny, a $k_{d,2}$ of ~1–2 kcal/mol seems most appropriate. To accurately represent the conformational preferences in biphenyl itself, it is likely that ortho hydrogens would need to be explicitly included. Since we found (see below) reasonable biphenyl angles, particularly for the cation complexes, we feel our simple model is satisfactory for our purposes.

As noted,[5] the calculations are most sensitive to the electrostatic parameters employed. As previous in 18-crown-6, we used ϵ = 1 throughout and a charge on the anisole oxygen of −0.6 and that of the carbons bonded to it 0.3, exactly analogously to what was used in cation complexes of 18-crown-6.[5] Elsewhere, we have shown[13] that an anisole –O– in which the O–CH_3 bond is perpendicular to the aromatic ring has properties quite like an aliphatic sp^3 oxygen, and this is further justification for the use of analogous partial charges. For simplicity, we used zero charges on the remaining atoms. For Na^+ and K^+, we used +1.0 charges and the van der Waals parameters previously employed, but we needed Li^+ parameters in this study. A value of α = 0.2 Å^3, slightly smaller than that for Na^+, and N_{eff} = 3 electrons were used in calculations on Li^+···OH_2, exactly as we have previously done for Na^+ and K^+. Only varying R_i^0, we arrived at a value (1.0 Å) that gave very good agreement with both the minimum energy distance (1.87 Å calculated, 1.81 Å accurate ab initio calculation)[15] and interaction energy ($-\Delta E$ = 34.9 kcal/mol compared to accurate ab initio values[15] of −35.0 and $-\Delta H_{exp}$[16] = −34.0).

Results

We used TEMPLATE[17] (a distance geometry based algorithm) to construct an initial geometry of M^+/**1**; we put distance geometry constraints of 2.0 Å on each metal–oxygen distance and values of 90° and 270° for the dihedral angles of the anisole methyl groups around the ring. The output of TEMPLATE had these methyl groups "up, down, up, down, down, up", so we broke one of the bonds connecting the aromatic rings and, using CHEM,[18] changed torsional angles to give the "up, down, up down, up down" orientation of the methyl groups observed in the X-ray structure.[4]

We then energy refined this structure with Li^+, Na^+, and K^+ parameters for the cation and then removed the cation and energy refined. Table II contains the energies and relative energies for such refinements, and Figures 1 illustrates the Li^+/**1** structure. The relative ΔE values are not surprising, with the complexation energies ($-\Delta E$) in the order $Li^+ > Na^+ > K^+$. What is impressive is the difference between $-\Delta E$ for Na^+ and K^+ (40.6 kcal/mol); the corresponding difference in the 18-crown-6 calculations with Na^+/C_1 symmetry 18–6 and K^+/D_{3d} symmetry 18–6 is 8.1 kcal/mol.[5] This enormous difference is also reflected in the metal–ligand energy ΔE_{ML}. Comparison of the complexation energy of **1a** and **1b** (Table II) shows that, as expected, the *p*-CH_3 groups have little effect on this energy. It is also surprising that the total energy of **1** is rather insensitive to the partial charge on oxygen, in contrast to 18-crown-6 (**4**). The relative orientation of the negative oxygens and the positive carbons to which the oxygens are attached are obviously different enough in **1** and **4** to cause a very different dependence of total energy on the partial charges.

Cram et al.[1,2] have shown that there is a dramatic difference in Li^+ and Na^+ affinity of **1** vs. **2**, so we studied **2** and its Li^+, Na^+, and K^+ complexes by removing an O–CH_3 group from the refined structures of **1** and M^+/**1** and energy refining **2** and M^+/**2**; the results are presented in Table III and Figure 2. The

Table II. Total and Interaction Energies for Li^+, Na^+, and K^+ Complexes with **1**

molecule	E_T[a]	ΔE[b]	ΔE_{ML}[c]	ΔE_L[d]
1b	76.3 (76.1)[e]			
Li^+/**1b**	−68.6	−144.9	−181.7	+36.8
Na^+/**1b**	−45.7	−122.0	−143.2	+21.2
K^+/**1b**	−5.1	−81.4	−95.8	+14.4
1a	69.7			
Li^+/**1a**	−74.9	−144.6		

[a] All energies in kcal/mol. [b] Complexation energy for $M^+ + 1 \rightarrow M^+$/**1**, using oxygen charge of −0.6 for both **1** and M^+**1**. [c] The metal ligand (ML) interaction energy calculated within the M^+/**1** complex. [d] $\Delta E - \Delta E_{ML}$; this is related to the "strain" induced in the ligand due to the metal–ligand interaction. [e] Total energy of **1b** with q_0 = −0.4, q_c = +0.2.

(14) The gas-phase angle in biphenyl is 42° (Almenningen, A.; Bastianson, O. *Kgl. Norske Vidnskab. Selskabs. Skrifter*, **1958**, *4*) and solvation effects on this angle are described by Birnstock [Birnstock, F.; Hoffmann, H.; Köhlrt, H. *Theor. Chim. Acta* **1976**, *42*, 311–323].

(15) Kistenmacher, H.; Popkie, H.; Clementi, E. *J. Chem. Phys.* **1973**, *58*, 1689.

(16) Dzidic, I.; Kebarle, P. *J. Phys. Chem.* **1970**, *74*, 1466.

(17) Weiner, P.; Profeta, S.; Wipff, G.; Havel, T.; Kuntz, I. D.; Langridge, R. *Tetrahedron* **1983**, *39*, 1113.

(18) CHEM, unpublished model building program written for the Evans and Sutherland Picture System 2 by A. Dearing (1981–1982).

Table III. Total and Interaction Energies for Li^+, Na^+, and K^+ Complexes with **2**

molecule	E_T[a]	ΔE[b]	ΔE_{ML}[c]	ΔE_L[d]	$\Delta\Delta E$[e]	$\Delta\Delta G$[f]	$\Delta\Delta G$[g]
2b	68.1						
Li^+/**2b**	−61.7	−129.8	−157.9	28.1	15.1	13.6	>12.6
Na^+/**2b**	−36.6	−104.7	−120.3	15.6	17.3	15.6	12.6
K^+/**2b**	1.6	−66.5	−81.6	14.9	14.9	12.9	*h*
2a	62.8						
Li^+/**2b**	−66.9	−129.7					

[a–d] See the corresponding footnotes of Table II. [e] Calculated energy difference between ΔE for M^+/**1** and M^+/**2** at 0 K, no vibration correction. [f] Calculated free energy difference between ΔG for association with M^+/**1** and M^+/**2**. [g] Experimental ΔG (association) differences for M^+/**1** and M^+/**2**. [h] No association observed.

Table IV. Vibrational Frequencies and Thermodynamic Parameters for **1**, **2**, and Their M^+ Complexes

molecule	vibrational frequencies[a]	ΔE[b]	ΔH[c]	ΔS[d]	ΔG[e]
1b	16.9, 20.0, 24.0, 39.4, 40.5, 41.7, 42.7, 49.0, 58.1, 68.8, 69.6, 73.6, 76.0, 76.6, 87.4				
Li^+/**1b**	49.8, 49.8, 51.8, 52.2, 61.3, 77.5, 77.5, 78.3, 85.4, 85.4, 87.8, 87.8	−144.9	−143.6	−46.6	−129.7
Na^+/**1b**	44.5, 44.5, 47.8, 50.7, 59.8, 59.8, 73.0, 77.6, 88.8, 88.8, 90.0, 90.0	−122.0	−121.2	−43.2	−108.3
K^+/**1b**	14.0, 40.3, 40.3, 57.8, 57.8, 66.9, 71.6, 79.8, 79.8, 82.9, 83.9, 83.9, 91.2, 91.2	−81.4	−83.3	−41.8	−69.9
2b	31.0, 32.5, 35.4, 41.2, 47.3, 51.2, 59.8, 62.3, 63.6, 74.7, 76.8, 77.2, 80.0, 96.0				
Li^+/**2b**	43.0, 44.6, 57.5, 65.1, 67.5, 71.9, 76.4, 83.4, 92.1, 94.8, 97.4	−129.8	−128.3	−41.0	−116.1
Na^+/**2b**	41.6, 42.0, 43.6, 54.6, 58.5, 64.1, 67.3, 68.7, 78.4, 85.1, 86.0, 88.8, 91.0	−103.7	−104.6	−36.8	−92.7
K^+/**2b**	23.4, 37.5, 39.9, 55.8, 57.2, 57.8, 73.1, 73.2, 78.5, 82.0, 82.5, 90.2	−66.5	−65.8	−35.0	−55.4

[a] Calculated vibrational frequencies less than 100 cm^{-1} in units of cm^{-1}. [b] Calculated ΔE at 0 °K (minimum energy geometry) (kcal/mol) for reaction M^+ + (**1** or **2**) → M/(**1** or **2**) with no vibrational correction. [c] Calculated ΔH^{298} with use of standard formulas for vibrational, rotational, and translational contributions to the enthalpy and the ideal gas approximation (kcal/mol). [d] Calculated ΔS^{298} with use of standard formulas for vibrational, rotational, and translational contributions to the entropy and the ideal gas approximation (cal/(mol deg)). [e] $\Delta G = \Delta H - T\Delta S(T = 298$ K), kcal/mol.

agreement between $\Delta\Delta E(M^+/\mathbf{1}$ vs. $M^+/\mathbf{2})$ and $\Delta\Delta G$ for the corresponding experimental measure is reasonable, given the simplicity of our model. Both the calculations and the experiments show that the removal of one $O-CH_3$ group causes a dramatic decrease in affinity (experimentally K_a decreased by $\sim 10^9$) due to the fact that one cation–oxygen interaction has been lost. Even in solution, the geometry of **2** would not permit a solvent molecule to replace the $-OCH_3$ removed when **1** is changed to **2**.

The ability to calculate normal modes of vibration lets us estimate the entropy and, thus, the free energy for the gas-phase reactions of M^+/**1**,**2**, and Table IV contains the results of such studies. In this table, we present the low-frequency vibrations ($\nu < 100$ cm^{-1}) as well as the ΔS, ΔH, and ΔG of complexation. Even though the calculated $\Delta\Delta S(M^+/\mathbf{1}$ vs. $M^+/\mathbf{2})$ explains some of the quantitative discrepancy between the calculated $\Delta\Delta E$ and the experimental $\Delta\Delta G$, the calculated $\Delta\Delta G$ is still slightly larger in magnitude than experiment, and, in contrast to experiment, $/\Delta\Delta G/$ is calculated to be larger for Na^+ than Li^+. The calculated vibrational frequencies themselves are of some interest. The lowest frequencies in **1b** are mainly "breathing" modes of OCH_3 groups, whose frequencies are raised by the presence of M^+, with the tightest binding cation Li^+ having the largest effect on the frequencies.

It was also of interest to simulate the reaction pathway for cation association to **1**. We thus used CHEM[18] to move M^+ approximately along the threefold axis of **1** to be as close as possible to equidistant to three of the oxygen atoms ($R \simeq 2.05$ Å), a point also equidistant to the other three oxygen atoms ($R \simeq 3.05$ Å). We than restrained the six $M^+\cdots O$ distances to these distances with a harmonic restraint potential ($K = 100$ kcal/(mol Å^2)) and energy refined the system for $M^+ = Li^+$, Na^+, and K^+; we then removed the restraint potential and re-refined the energy. Finally, we used CHEM[18] to move M^+ 1 Å further along the threefold axis than the point closest to three of the oxygens, so that it was *outside* the cavity of **1** and energy refined. The results of these studies are summarized in Table V. In the calculations with the cation constrained to stay approximately at the center of the three oxygens, the energy costs for $M^+ = Li^+$ and Na^+ are remarkably similar, 25.4 and 25.8 kcal/mol, respectively, whereas the energy cost for $M^+ = K^+$ is 55.4 kcal/mol. With the restraint removed, all three ions return to the center of the cavity. When one starts M^+ outside the cavity with no restraints, $M^+ = Li^+$ or Na^+ return to the center, with an energy 18.1 kcal/mol lower than that at the threefold axis in the plane of the three oxygens. It should be emphasized that we did not start the M^+ or restrain it precisely along the threefold axis, so that if lower symmetry pathways for association existed for K^+, there was no intrinsic restriction to prevent the ion from finding them. We also rotated each of the three anisole $-CH_3$ groups from their initial dihedral angles ca. perpendicular to the ring to ~60° so that the M^+ ions would "see" more of the oxygens as the refinement began, but this led to identical results as no rotation (Li^+, Na^+ forming an "inclusive" complex with **1**, K^+ forming an "exclusive" complex).

Table V. Total Energies for "Reaction" Pathway Calculations of M^+/**1** Complexes

complex	E_r(center)[a]	E_r(3-fold)[b]	E_T(3-fold, relax)[c]	E_r("outside")[d]
Li^+/**1**	−68.6	−43.2	−68.6	−68.6
Na^+/**1**	−45.7	−19.8	−45.7	−45.7
K^+/**1**	−5.1	50.3	−5.1	32.2

[a] Energy for M^+ in the center from Table II (kcal/mol). [c] Starting with geometry optimized with restraint described in footnote *b* and re-refined. All three metals refined to the original central position (note equivalence with 1st column (kcal/mol). [d] Starting with geometry 1 Å "outside" the entrance to the cavity along the 3-fold axis and refining with no restraint. Note that the Li^+ and Na^+ return to the center of the cavity; the K^+ does not. Energy in kcal/mol.

In Table VI we present the structural results for **1** and **2** and their complexes with Li^+, Na^+, and K^+, for comparison, in the case of **1**, with the X-ray results of ref 4. The average $\phi-\phi$ dihedral angles for Li^+/**1** and Na^+/**1** are in excellent agreement with experiment; for **1** itself, the average calculated $\phi-\phi$ angle is ~22° too large. The reason for this latter discrepancy is not clear. The inclusion of an explicit torsional potential, $K_{d,2} = 1.5$ kcal/mol, for the biphenyl barrier led to a decrease in average $\phi-\phi$ angle of **1** of only 3°. Thus, given the insensitivity of the spherand structures to the torsional barriers, a zero barrier was used in all the remaining calculations as we have noted in Methods (Table I).

Spherand **3a** differs from **1** in the addition of a single $-CH_2-$ group connecting meta $O-CH_3$ groups. Its experimental Li^+ affinity is roughly halfway between that of **1** and **2**, but its structure contains very close oxygen···oxygen distances (2.5 Å) between the meta oxygens which are part of the $O-CH_2-CH_2-CH_2-O$ fragment but not connected by the bridge. Because of these close contacts, one expects that the net oxygen charge on the four bridge oxygens will be reduced because the electric field

Table VI. Calculated and Experimental Geometrical Parameters for **1**, **2**, and Their M^+ Inclusion Complexes[a]

molecule	$R(O\cdots O)_{ortho}$[b]	$R(O\cdots O)_{meta}$[c]	$R(O\cdots O)_{para}$[d]	$\phi(Ar\cdots Ar)$[e]	$\phi(OCH_3)$[f]	$\phi(COCH_3)$[g]	$R(M^+\cdots O)$[h]
1	3.55 (2.92)	3.89 (3.32)	5.24 (4.42)	73.6 (52)	84.2 (62)	116.5 (115)	
Li^+/**1**	2.74 (2.78)	3.21 (3.24)	4.22 (4.28)	55.1 (56)	87.1 (85)	112.6 (112)	2.11 (2.14)
Na^+/**1**	3.02 (3.00)	3.44 (3.43)	4.66 (4.55)	62.3 (61)	86.9 (84)	114.0 (113)	2.33 (2.28)
K^+/**1**	3.57	3.88	5.31	83.4	86.3	114.6	2.66
2	3.51	4.03	5.22	80.9	81.6	116.4	
Li^+/**2**	2.74	3.20	4.06	63.1	85.7	112.2	2.05
Na^+/**2**	3.03	3.47	4.48	68.2	86.8	113.6	2.30
K^+/**2**	3.49	4.01	5.22	79.8	86.4	114.2	2.61

[a] Experimental values (where available) from ref 4 in parentheses; calculations on **1b** and its complexes; experiments on **1a** and its complexes. [b] Average distance between pseudo-ortho oxygens (Å). [c] Average distance between pseudo-meta oxygens (Å). [d] Average distance between pseudo-para oxygens (Å). [e] Average dihedral angle of aryl groups (deg). [f] Average dihedral angle of OCH_3 with respect to aryl (deg). [g] Average Ar–O–CH_3 angle (deg). [h] Average $M^+\cdots O$ distance (Å).

Table VII. Results of Simulations on **3a**, **3b**, and Their Li^+ and Na^+ Complexes

molecule	E[a]	ΔH[b]	ΔS[c]	ΔG[d]	$\Delta\Delta G_{calcd}$[e]	$\Delta\Delta G_{exptl}$[f]
3a	111.0					
Li^+/**3a**	−19.6	−129.2	−26.4	−121.3	8.4	7.2
Na^+/**3a**	2.8	−107.2	−29.7	−98.3	10.0	5.6
3b	70.4					
Li^+/**3b**	−89.5	−158.2	−39.7	−146.4	−16.7	
Na^+/**3b**	−61.4	−130.5	−41.8	−118.1	−9.8	

molecule	vibrational frequencies[g]
3a	27.9, 47.2, 56.9, 64.7, 72.3, 81.7, 89.5, 91.5
Li^+/**3a**	23.7, 27.5, 44.9, 46.7, 58.6, 61.8, 77.8, 98.9
Na^+/**3a**	22.7, 45.8, 52.2, 55.0, 55.8, 75.4, 93.7, 98.1
3b	29.3, 38.5, 46.3, 47.2, 55.0, 60.3, 64.7, 74.0, 75.9, 88.8, 91.4
Li^+/**3b**	41.8, 54.7, 58.5, 69.1, 79.0, 88.0, 89.4, 90.1
Na^+/**3b**	46.1, 54.2, 54.8, 66.6, 67.1, 79.0, 88.0, 89.4, 90.1

	structural parameters						
molecule	$R(O\cdots O)_{ortho}$[h]	$R(O\cdots O)_{meta}$[i]	$R(O\cdots O)_{para}$[j]	$R(M^+\cdots O)$[k]	$\phi(Ar\cdots Ar)$[l]	$\phi(OCH_3)$[m]	$\theta(COCH_3)$[n]
3a	3.25 (4), 2.46 (2)	4.65 (4), 3.21 (2)	4.76 (1), 4.03 (2)		12 (2), 66 (4)	60	119.0
Li^+/**3a**	2.69 (4), 2.41 (2)	4.06 (4), 2.93 (2)	4.00 (1), 3.80 (2)	2.60 (1), 2.05 (5)	8 (2), 57 (4)	70	114.3
Na^+/**3a**	2.83 (4), 2.40 (2)	4.27 (4), 3.01 (2)	4.25 (1), 3.85 (2)	2.30	0 (2), 62 (4)	68	114.1
3b	3.10 (4), 2.95 (2)	3.56 (4), 3.21 (2)	5.07 (1), 4.34 (2)		70	66	118.9
Li^+/**3b**	2.74	3.31 (4), 3.01 (2)	4.52 (1), 4.04 (2)	2.27 (2), 2.02 (4)	62	72	114.1
Na^+/**3b**	2.98	3.46 (4), 3.19 (2)	4.50	2.25	67	65	116.2

[a] Total energy in kcal/mol. [b] Enthalpy difference in kcal/mol at 298 K between **3** and its M^+ complexes. [c] Entropy difference in cal/(mol deg) at 298 K between **3** and its M^+ complexes. [d] Free energy difference in kcal/mol at 298 K between **3** and its M^+ complexes. [e] Free calculated energy difference in M^+ association between this compound and **1** (kcal/mol). [f] Experimental free energy difference in M^+ association between this compound and **1** (kcal/mol). [g] All vibrational frequencies less than 100 cm^{-1} in cm^{-1}. [h] Average distances between pseudo-ortho oxygens (Å); in the case of two numbers, the number of O···O distances contributing to each average is given in parentheses. [i] Average distances between pseudo-meta oxygens (Å). [j] Averge distances between pseudo-para oxygens (Å). [k] $M^+\cdots O$ distances in Å. [l] Average phenyl–phenyl dihedral angle; values in parentheses refer to the number of dihedral angles contributing to the average (deg). [m] Average $CCOCH_3$ dihedral angle (deg). [n] Average $COCH_3$ angle (deg).

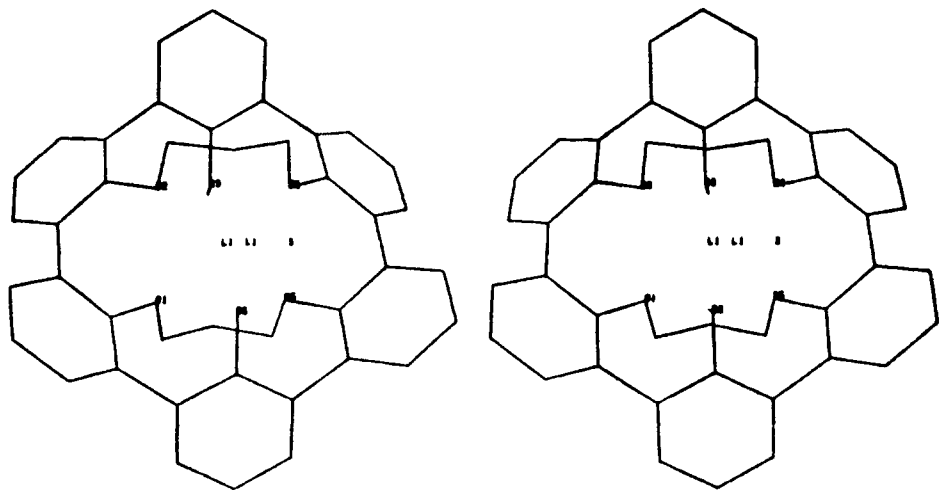

Figure 3. Stereo drawing of energy-refined Li^+/**3a**.

on one oxygen will induce a dipole with polarity opposite to that induced by a metal cation. Calculations on the magnitude of the polarization due to the cation electric field in 18-crown-6 showed that such a polarization of the oxygen caused a change of its charge (q_0) from −0.3 to −0.6 by Na^+, K^+, Rb^+, Cs^+ at $R(M\cdots O) \sim$ 2.5–3.0 Å. Given that one has a dipole of ~1 au at approximately the same distance of 2.5 Å, one would expect ~1/2.5 the induced dipole due to nearby –O– dipoles on each bridge –O–. This suggested that one should use $q_o = -0.5$, $q_c = 0.25$ for the four bridged oxygens and the adjacent carbon atoms in **3a** and $q_o =$

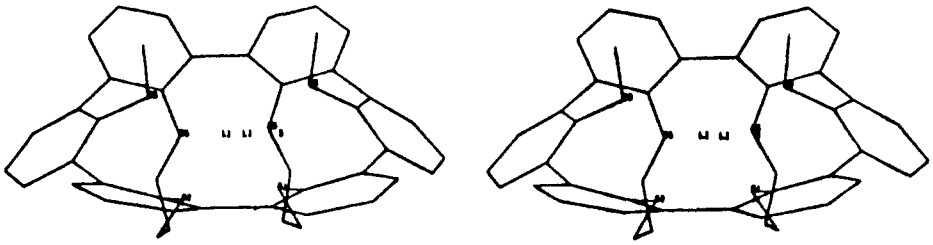

Figure 4. Stereo drawing of energy-refined Li^+/**3b**.

−0.6, q_c = 0.3 for the two methoxyl groups and their adjacent carbon atoms, as we had for the similar groups in **1**. Again, we generated the structure of **3a** using the template-driven distance geometry and energy refined the resulting structure. Table VII and Figure 3 contain the results of energy refinements on **3a** and Li^+/**3a**; as one can see, the calculated $\Delta\Delta G$ (relative to Li^+**1**) is +8.4 kcal/mol, in reasonable agreement with the experimental value of >7.2 kcal/mol. The Na^+/**3a** calculated $\Delta\Delta G$ (relative to Na^+/**1** is 10.0, compared to 5.6 kcal/mol found experimentally. Given our crude estimate of atomic partial charges, these $\Delta\Delta G$ are certainly reasonable.

In the process of model building **3a**, we asked ourselves the following: why should **3a** not adopt conformation **3b**, in which the oxygens are alternating as in **1**? We thus used the template driven distance geometry approach to generate structure **3b**, which was then energy refined (Figure 4). The molecular mechanics calculation suggested that **3b** was more than 40 kcal/mol lower in energy than **3a** and its Li^+ complex nearly 70 kcal/mol lower in energy. Thus, our prediction is that **3b**, if synthesized, will have the highest Li^+ affinity yet determined.

One immediately asks the following question: if **3b** is so much more stable than **3a**, why is it not found? The mechanisms of the "template driven" radical syntheses of **1**–**3** are not well understood, but if **3a** is the kinetically favored product, it may have difficultly isomerizing to **3b**. We attempted to model build and carry out constrained refinements of the **3a** ⇄ **3b** transition state and never found a transition-state model lower than 50 kcal/mol above **3a**; it is very difficult to slide an O–CH_3 group "underneath" the O–CH_2–CH_2–CH_2–O chain, as must be done to go from **3a** → **3b**. Thus, we concur with the idea that **3a** is kinetically stable relative to isomerization to **3b**; however, the results of our calculations also strongly encourage the search for reaction conditions which will result in **3b**.

Given that we made no assumption about the orientation of the Li^+ in Li^+/**3a**, starting the optimization in a roughly central location, it should be considered a qualitative validation of our approach that the refined Li^+/**3a** complexes contain five Li^+···O distances which average 2.05 Å and one long Li···O distance of 2.60 Å (Figure 3). The experimental X-ray structure[2] has 5 Li^+···O distances between 2.00 and 2.09 Å and one Li^+···O distance of 2.99 Å. The calculated Na^+/**3a** complex on the other hand has all six M^+···O distances near 2.3 Å.

There are also interesting differences in the vibrational properties of **3a**, **3b**, and their M^+ complexes (Table VII). **3b** is like **1**, in that its M^+ complexes have higher frequencies than the uncomplexed structure, even though its lowest frequencies are higher than for **1**, due to the $-CH_2-$ bridge restraining O···O breathing. **3a** on the other hand is more highly constrained and has fewer modes <100 cm^{-1}, and Li^+ or Na^+ binding leads in most modes <100 cm^{-1} to a lowering of the frequencies. The lowest modes in these M^+/**3a** complexes have significant M^+···O character. The higher frequencies and more constrained nature of **3a** compared to **3b** are also reflected in their relative absolute entropies and relative ΔS values for cation association (Table VII).

Discussion

An interesting result found here is the ~40 kcal/mol difference in affinity of Na^+ vs. K^+ for **1**. This is nicely consistent with the very favorable Na^+ binding free energy that Cram et al.[2] observed for **1** ($-\Delta G$ = 19.2 kcal/mol) but the lack of any observable K^+ affinity of **1**. We also suggest that part of the lack of K^+ affinity of **1** may be kinetic, since our calculations show an intrinsic barrier for K^+ to enter **1** but no barrier for Li^+ or Na^+ entrance into **1**. Any intrinsic activation energy for Na^+ or Li^+ association with **1** comes from the need to "desolvate" the cation prior to entering **1** rather than any barrier to entering, as suggested by the definitive kinetic and thermodynamic studies of cation association to **1** of Lein and Cram.[3] In the case of K^+, both desolvation and the entrance barrier must be surmounted simultaneously and thus our calculated activation energy of ~18 kcal/mol, for K^+ entering the spherand along the threefold axis, is likely a lower bound to the true free energy of activation.

Cram et al.[1] note that **1** in $CDCl_3$ extracts Na^+ more rapidly than Li^+ from D_2O but will not extract K^+, Mg^{2+}, Ca^{2+}, and Sr^{2+}. The likely reason why **1** does not extract divalent cations (and this reason may partially explain the lack of K^+ affinity) is that it does not afford the cation–second-shell interactions found in aqueous solution. Thus, an improvement of **1** might attempt to build in such interactions, such as are present in spherical cryptands where 6 ether–O groups aid the 4 nitrogen lone pairs in attracting cations.[19] We suggest that the faster rate of association to **1** for Na^+ than Li^+ is indeed due to the slower desolvation of H_2O from Li^+, its ΔG hydration being −124 kcal/mol compared to −98 kcal/mol for Na^+.[20] It is also interesting that this hydration energy difference of 26 kcal/mol is qualitatively similar to our calculated interaction energy difference of 23 kcal/mol for Li^+/**1** compared to Na^+/**1**, consistent with the comparable and high affinity of both Li^+ and Na^+ for **1**. On the other hand, the calculated difference in interaction energy of Na^+/**1** and K^+/**1** is ~40 kcal/mol, far greater than the differences in hydration free energy[20] of ~18 kcal/mol. As noted previously, we calculate that there is a many order of magnitude thermodynamics of Na^+/**1** over K^+/**1**, consistent with the lack of experimental observation of the latter. The K^+/**1** complex *might* be observable, but only under conditions in which one can strip away its hydration shell and be at high enough temperatures to surmount the intrinsic barrier to association. The lack of observation of $Mg^{2/}$**1** and Ca^{2+}/**1** has been interpreted[1] as kinetic; we concur that there should be a much larger barrier to desolvating these divalent cations to allow association with **1** than for the comparable size monovalent cations Li^+ and Na^+. There may be an appreciable thermodynamic reason as well for the lack of affinity of divalent cations for **1**, since the contribution to the net hydration enthalpies from the waters outside the first hydration shell are clearly more important for divalent ions;[19] in **1**, no such second or further shells of hydrophilic O atoms exist. In the above analysis, we have attempted to relate our calculated energies for M^+(Li^+,Na^+,K^+) complexation of **1** to the experimental energetics of the reaction

$$M^+(H_2O)_n + \mathbf{1} \xrightarrow{\Delta G} M^+/\mathbf{1} + (H_2O)_n$$

We note that to compare ΔG for one ion with that of the other requires a knowledge of both the intrinsic ΔG for M^+/**1** complex formation and the *relative* solvation energies of M^+ (taken from experimental data). Although such a hydrid approach is quite

(19) Graf, E.; Kintzinger, J. P.; Lehn, J. M.; Le Moigne *J. Am. Chem. Soc.* **1982**, *104*, 1672.
(20) See: Friedman, H. In "Watger, A Comprehensive Treatise"; Franks, F., Ed.; Plenum Press: New York; Vol. 3, Chapter 1, pp 1–113.
(21) Kollman, P.; Kuntz, I. *J. Am. Chem. Soc.* **1972**, *94*, 9236.
(22) Cram, D. J.; Kaneda, T.; Sein, G. M.; Helgeson, R. C. *J. Chem. Soc., Chem. Commun.* **1979**, *848*.

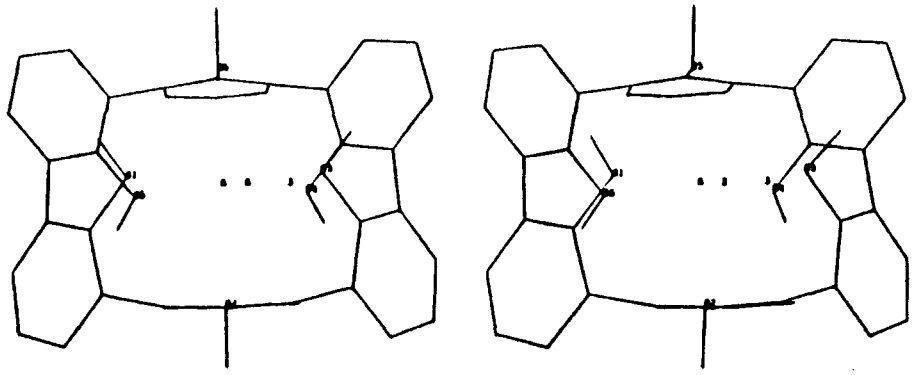

Figure 5. Stereo drawing of energy refined K^+/**1b**.

crude, the difference between the affinity of Li^+ and Na^+ vs. that of K^+ for **1** noted above is so large it is unlikely to be calculation model dependent.

The simplest physical explanation why K^+ is so weakly bound by **1** would to its too large size. This introduces ligand strain, and at the same time, short O···K^+ interactions reduce the net attractive interactions (due to the $^1/_{R^{12}}$ exchange repulsion energy term) (see Figure 5). However, this explanation does not hold up under closer scrutiny. If one compares the ligand strain energies ΔE_L induced by cation association, one fines that Na^+ induces about 7 kcal/mol more strain energy than K^+ when associating with **1** (Table II). This difference is actually quite comparable to that in 18-crown-6, where the corresponding difference for the D_{3d} conformation is 8 kcal/mol.[5] The reason for the profound difference between Na^+ and K^+ affinities for spherand **1** is that *both* cations are capable of interacting with this molecule nearly six times as strongly as the single dimethyl ether molecule is. The calculated interaction energy ($-\Delta E$) for $M^+ + O(CH_3)_2$ complex is 25.6 kcal/mol for Na^+ and 18.2 kcal/mol for K^+.[4] The $-\Delta E_{ML}$ values for Na^+/**1** and K^+(**1**) are 143 and 96 kcal/mol, respectively, quite near to the optimal one could expect of 6× the single dimethyl ether value. If one looks at the X-ray O···O para distance in **1** (Table VI) (2.21 Å), one notes that **1** is approximately the right size for Na^+, but our calculations suggest that it can adapt to the size of K^+ without much strain. However, if each M^+···O interaction is ~8 kcal/mol stronger for Na^+ than K^+, this leads to a very large difference in ΔE_{ML}, which is not found in 18-crown-6. In 18-crown-6, the six oxygens are very far from an optimal alignment for either Na^+ or K^+, so any intrinsic differences in cation···O interactions are damped out. In addition, the lowest energy cation binding conformation of 18-crown-6 (D_{3d}) is about the right size for K^+ binding (2.7–2.8 Å) and shrinks rather little when Na^+ is placed into this conformation. That is why Na^+ prefers[4] the distorted C_i conformation of 18-crown-6, which has about a 16 kcal/mol more favorable crown/cation energy but a ~12 kcal/mol higher strain energy.

One views 18-crown-6 as more flexible than spherand **1**, because it can adopt so many more conformations. However, the fact that the oxygens in **1** are not part of the macrocyclic ring enable it to align its dipoles very effectively toward the cation, something 18-crown-6 cannot do as well because all its –O– groups are tried to the single ring. Even in **3**, the $-O-CH_2-CH_2-O-$bridge can be somewhat flexible and not affect the biphenyl ring conformation.

One could make the argument that spherand **1** is so much a better binding ionophore than 18-crown-6 (**4**), because its lowest energy conformation in the absence of cation is very similar to its cation binding conformation, and, thus, the spherand need pay a much lower enthalpic and entropic price for binding a cation. This is certainly the predominant effect when 18-crown-6 adopts the C_i conformation observed in crystal studies of Na^+/**4**. However, the D_{3d} conformation is calculated to be only 1.1 kcal/mol higher in energy than the lowest energy C_i conformation of **4** and the entropy price on binding a cation would be larger than for **1**, but such an effect would only correspond to a free energy cost of 1–2 kcal/mol. Because of the ring contraint, even the D_{3d} conformation of 18-crown-6 does not have the near ideal ion-binding conformation of **1**. We conclude that there are two important reasons why **1** is such an effective ionophore: first, it has a near ideal, "ion-binding" conformation in the absence of cation, and second, the fact that its $R-O-CH_3$ ion binding groups are not part of the macrocyclic ring facilitates further optimization of cation–ionophore interactions.

Another interesting puzzle is why aqueous K^+ associates with 18-crown-6 (**4**) but not with **1**, given that the calculated gas-phase M^+ interaction energies are 73.6 and 81.4 kcal/mol, respectively. The most reasonable explanation seems that K^+/**4** can associate with further water molecules; as shown in ref 5, the net interaction energy of K^+ with **4** and two water molecules is 86.4 kcal/mol. In **1**, the K^+ is buried inside the cavity and waters or counterions must be far away.

Given the simplicity of our model, one should consider the qualitative agreement between the calculated $\Delta\Delta E$ and $\Delta\Delta G$ for M^+/**1** vs. M^+/**2** (14–17 kcal/mol) and the experimental value (12–13 kcal/mol) reasonable. It makes sense that the solution-phase value should be smaller than the gas-phase value. This is because any residual ion pairing of M^+ with its counterion in solution will be stronger for **2**; the absence of one $O-CH_3$ group will allow a closer approach of the anion to the M^+/**2** than to the M^+/**1** complex. This will stabilize M^+/**2** relative to M^+/**1** and reduce the calculated intrinsic difference in stabilization energies.

The most exciting result of these calculations is the prediction that **3b** should give the highest Li^+ affinity known. After doing the calculation on this isomer, we returned to the literature to ref 20, in which Cram et al. had, prior to the X-ray structure done in ref 2, suggested that **3** would have conformation **3b**. Our studies on the **3a** ⇄ **3b** reaction pathway convinced us of the extremely high barrier between these isomers. Thus, we hope these calculations will provide a renewed stimulus for further attempts to synthesize **3b**, since its properties are so interesting.

A referee has noted that a previous version of this manuscript gave the "impression that the authors are applying thoroughly tested standard procedures to get chemically valid results". We do not wish to leave the impression that the study of ion–neutral complexes with molecular mechanics has been shown to "routinely" give a quantitative representation of the energetics of association. The spherands studied here are a particularly fortunate class of molecules for theoretical calculations because their highly constrained nature makes the "local minimum" problem so much less severe. However, we feel that the successful application of molecular mechanics to both 18-crown-6 (**4**) and the spherands with essentially the same theoretical model is not entirely fortuitous. Such a model has involved calibration of parameters with gas-phase data and quantum mechanical calculations on cation–water and dimethyl ether interactions.

This referee has also questioned the use of the simple force field employed here to calculate the vibrational frequencies of molecules, since this force field has not been calibrated to reproduce experimental vibrational data. We stress that the major use of the frequencies has been to enable the calculation of ΔG's rather than ΔE's of complexation, but all of the qualitative conclusions reached there would be the same if one considered ΔE's rather than ΔG's.

We feel justified in presenting the ΔG values for two reasons: (1) The differences between ΔG and ΔE are dominated by the ΔS term and the compensation between the translational/rotational entropy loss and the entropy in the low frequency (<100 cm^{-1}) normal modes. There is precise information on these modes for very few molecules. Thus, calibration to experiment for these low modes would be impossible. (2) There is indirect evidence, based on a comparison of our normal mode calculations on progesterone with a variety of simple and complex force fields,[23] that such low frequency modes are relatively insensitive to details of the force field, provided that qualitatively reasonable parameters are used.

Conclusion

The major conclusions of this study are the following: (1) We have further validated the power and utility of molecular mechanical methods in simulating the kinetics and thermodynamics of ionophore–cation interactions. With use of the same set of parameters successfully applied to study 18-crown-6 (**4**), the calculations have rationalized the very different cation selectivity of **1** and **4** and the dramatically different cation affinities of **1** and **2**, as well as suggesting differences in kinetics of K^+ and Na^+ association to **1**. (2) The calculations used *no X-ray structural data*, per se, as input, illustrating the power of a distance geometry/computer graphics/molecular mechanics approach to studying molecular interactions in complex systems. A subsequent comparison of the calculated structures with the available X-ray structures of the ionophore–carbon complexes reveals satisfactory agreement, even in the case of Li^+/**3a**, where both the calculated and experimental structures find 5 short and 1 long Li···O distances. (3) The combined use of these different theoretical approaches has also enabled us to charcterize the properties of a new isomer of **3**, **3b**, which has been predicted to have the highest known Li^+ and Na^+ affinities.

Acknowledgment. P.A.K. and G.W. are pleased to ackowledge the support of a NATO travel grant (0478/82) in this research. P.A.K. thanks Ken Trueblood for bringing these molecules to his attention, both Ken Trueblood and Donald Cram for useful comments, and the NIH (GM-29072) for research support. The facilities of the UCSF Computer Graphics Lab, supported by NIH-RR-1081 (R. Langridge, director, and T. Ferrin, system manager), were essential to the success of this study.

Note Added in Proof. R. C. Helgeson and D. J. Cram (private communication) have succeeded in preparing and characterizing **3b** and Li^+/**3b**. They have found that Li^+ is more difficult to decomplex from **3b** than from **1**, which appears to verify our prediction.

Registry No. 1a, 72526-85-3; **1b**, 95045-92-4; **2a**, 80109-06-4; **2b**, 95045-93-5; **3**, 95045-94-6; Li, 7439-93-2; Na, 7440-23-5; K, 7440-09-7.

(23) Kollman, P.; Murray-Rust, P.: normal mode calculations on progesterone at both the all atom and united atom level, using force field parameters from ref 6 and 9–10.

Simulation of Formamide Hydrolysis by Hydroxide Ion in the Gas Phase and in Aqueous Solution

Scott J. Weiner, U. Chandra Singh, and Peter A. Kollman*

Contribution from the Department of Pharmaceutical Chemistry, University of California, San Francisco, California 94143. *Received May 9, 1984*

Abstract: We present the results of a new approach for simulating chemical reactions by using quantum mechanical and molecular mechanical methods. This approach is applied to the hydrolysis of formamide by hydroxide ion. In the gas phase, tetrahedral complex (TC) formation is calculated to proceed with no barrier and TC breakdown involves a small barrier (12 kcal/mol). In solution, we calculate a 22-kcal/mol barrier for *formation* of the TC with a second, smaller barrier occurring for TC breakdown. The calculated reaction energies and activation energies are in quite good agreement with available experimental data.

The mechanisms by which enzymes catalyze chemical reactions have intrigued theoretical chemists and biochemists for years.[1-4] Warshel and Levitt's pioneering approach to simulating enzymatic reactions,[5] and the application of this approach to lysozyme cleavage of saccharide linkages, was the first study which combined the environmental and internal strain factors by using a molecular mechanical model with semiempirical quantum mechanical techniques to evaluate the energetics of bond breaking. The results of their calculations were encouraging and showed the dramatic effects that electrostatic interactions have in stabilizing the intermediate carbonium ion in this reaction. Although their method has much merit, we feel that recent developments in ab initio quantum mechanical theory[6] and accurate potentials for liquid water[7] make it a propitious time to develop another approach for simulating enzymatic reactions.

With this in mind, we present a method for simulating noncatalyzed, as well as enzymatic reactions, in aqueous solution. This method can best be broken down into two very general steps: the use of ab initio quantum mechanics to evaluate bond breaking energies and molecular mechanics for calculating the remaining energies, dominated by strain and noncovalent interactions. The solute(s) is completely surrounded by explicit water molecules, taken from a Monte Carlo simulation on liquid water,[8] and allowed to energy-refine by using molecular mechanics. As our first

(1) General reviews: Walsh, C. In "Enzymatic Reaction Mechanisms"; W. H. Freeman: San Francisco, 1979. Fersht, A. In "Enzyme Structure and Mechanism"; W. H. Freeman: San Francisco, 1977.
(2) Wipff, G.; Dearing, A.; Weiner, P.; Blaney, J.; Kollman, P. *J. Am. Chem. Soc.* **1983**, *105*, 997.
(3) Scheiner, S.; Lipscomb, W. *Proc. Natl. Acad. Sci. U.S.A.* **1976**, *73*, 432.
(4) Van Duijnen, P.; Thole, B.; Hol. W. *Biophys. Chem.* **1979**, *9*, 273.
(5) Warshel, A.; Levitt, M. *J. Mol. Biol.* **1976**, *103*, 227.
(6) Binkley, J.; Whiteside, R.; Krishnan, R.; Seeger, R.; Defrees, D.; Schlegel, H.; Topiol, S.; Kahn, L; Pople, J. Gaussian BO, Indiana University, Bloomington, 1980.
(7) Jorgensen, W.; Chandrasekhar, J.; Madura, J. *J. Chem. Phys.* **1983**, *79*, 926.
(8) The Monte Carlo cube of 216 water molecules was kindly provided to us by W. Jorgensen.

0002-7863/85/1507-2219$01.50/0